LAPPEENRANNAN-LAHDEN TEKNILLINEN YLIOPISTO LUT
School of Engineering Science
Electrical Engineering

Joonas Ihalainen

PHASE-CHANGE COOLING IN ELECTRICAL MACHINES

Master's Thesis

Examiners: Prof. Juha Pyrhönen
D.Sc. Ilya Petrov

ABSTRACT

Lappeenranta-Lahti University of Technology LUT
School of Engineering Science
Degree Programme in Electrical engineering

Joonas Ihalainen

Phase-change cooling in electrical machines

Master's thesis
2022
36 pages, 13 figures, 2 tables and 1 appendix
Examiners: Professor Juha Pyrhönen and D.Sc. Ilya Petrov

Keywords: Phase change, cooling, heat pipe, electrical machine

This study highlights a few research papers published in the field of phase-change cooling of electrical machines. The study is mainly concentrated on the use of different kinds of heat pipes to cool either the rotor or the stator part of the electrical machine. Research concludes that heat pipes can be used to effectively cool electrical machines. However, there are numerous variables that affect the design and efficiency of the heat pipe cooling. These include heat pipe fluid inventory, tilt to the horizontal axis, ambient temperature, and heat pipe material.

TIIVISTELMÄ

Lappeenrannan-Lahden teknillinen yliopisto LUT
School of Engineering Science
Sähkötekniikan koulutusohjelma

Joonas Ihalainen

Faasimuutosjäähdytys sähkökoneissa

Diplomityö
2022
36 sivua, 13 kuvaa, 2 taulukkoa ja 1 liite
Tarkastajat: Professori Juha Pyrhönen ja TkT Ilya Petrov

Hakusanat: Faasimuutos, jäähdytys, lämpöputki, sähkökone

Työ korostaa muutamia aiempia tutkielmia faasimuutosjäähdytyksestä sähkökoneissa. Tutkielma käsittelee pääasiassa erityyppisten lämpöputkien käyttöä sähkökoneiden jäähdytyksessä. Lämpöputket osoittautuivat tehokkaaksi tavaksi jäähdyttää sähkökoneita. Lämpöputken jäähdytyskykyyn ja suunnitteluun vaikuttaa kuitenkin suuri määrä erilaisia muuttujia, kuten esimerkiksi lämpöputken täyttökerroin, sen kulma horisontaaliseen akseliin nähden, ympäröivä lämpötila, ja lämpöputken materiaali.

ACKNOWLEDGEMENTS

I want to thank my supervisors Prof. Juha Pyrhönen and M.Sc. Ilya Petrov for their patience and for providing guidance throughout this ordeal.

Special thanks to Lehmus Roastery for providing me quality coffee, which gave me solace and endurance needed in this arduous task.

Super special thanks to friends and family who managed to endure my stressed-out rants about writing my thesis over the course of my frankly long making of my thesis.

May 2022

Joonas Ihalainen

TABLE OF CONTENTS

LIST OF SYMBOLS AND ABBREVIATIONS

A	Area
A_{V}	Vapor core cross-sectional area
A_{W}	Wick cross-sectional area
h_{c}	Condenser heat transfer coefficient
h_{fg}	Latent heat of vaporization
L_{t}	Total length of heat pipe
M	Fluid inventory
r_{m}	Taper section mean radius
T	Temperature
$T_{\mathrm{c,av}}$	Average temperature of the condenser
T_{f}	Temperature of oil inlet
Q_{cal}	Removed heat energy
α	Half cone angle of the condenser taper
δ	Fluid film thickness
ε_{o}	Wick material porosity
ρ_{f}	Fluid density
ρ_{l}	density of liquid water
ρ_{V}	Vapor density
Ω	Mechanical angular velocity
GWP	Global warming potential
HSRHP	High-speed rotating heat pipe
ID	Inner diameter
OD	Outer diameter
OR-PM S/G	Outer-rotor permanent magnet starter/generator
PCM	Phase change material
PMSM	Permanent magnet synchronous machine
RHP	Rotating heat pipe
VCHP	Variable conductance heat pipe

1 INTRODUCTION

1.1 The principle of phase change cooling

The idea in phase-change cooling is to exploit the latent heat of a suitable cooling material when it goes through a phase change or phase changes for instance in a heat pipe. In other words when cooling an instalment with fluids, one can either exploit the latent heat of fusion or the latent heat of vaporization. In some cases, phase change from a solid to liquid and vice versa can also be used. During phase change the temperature of the cooling medium is close to being constant.

The phase change material (PCM) is then utilized as a thermal energy storage (Socaciu, 2012) or as a medium for heat transfer, like in heat pipes for instance. Solid PCMs at room temperature such as paraffin have been used in thermal energy storages. These thermal storages could be used in conjunction with periodic overloading of electrical machines to maintain overloaded windings at safe temperature (Xiong 2017).

1.2 Common cooling substances

Especially in heat pipes, many different cooling substances may be utilized. For instance, water, acetone, ammonia, R-134a, HFO-1234yf, etc. have been used in heat pipes as circulating fluid transmitting heat energy away from the working component. The properties of the most common cooling substances are studied in the following.

1.2.1 Water

Water is a great heat transferring medium with its large enthalpy of vaporization. Water heat pipes function best at the higher end of their temperature range. According to ACT (Advanced cooling technologies 2021) 25 °C is considered to be a rough bottom limit for a water heat pipe function. Below this point water heat pipe transfers heat mainly through conduction, which is not a problem when cooling conventional electronics, since the heat pipe will start operating once its temperature reaches the lower limit. However, in low temperature setting the possibility of water freezing in the heat pipe must be considered. If the heat pipe is properly designed, it can withstand thousands of freeze/thaw cycles, but if operation temperatures should be kept below 25 °C, a different working fluid such as methanol should be considered.

1.2.2 Methanol

Methanol is the simplest alcohol. It is light, volatile, colourless, and flammable. According to Cooling house Co. methanol heat pipe's operating temperature range is between −20 ℃ and +80 ℃. While in liquid form at ambient pressure and temperature its specific heat is 2.53 kJ/(kg·K), which is noticeably lower than that of water, its strengths lie in its capability to work in sub-zero temperatures. However, when it comes to cooling electrical motors, those temperatures are seldomly required.

1.2.3 Ammonia

According to Goddard Space Flight Centre (GSFC, 1999) published article, ammonia-charged aluminium heat pipes are applicable in most near-room temperature (200 K – 350 K) applications. In liquid form its specific heat is very high, 4.6 kJ/(kg·K).

However, Occupational Safety and Health Administration warns that ammonia is considered a high health hazard because of its corrosive nature. It is harmful to skin, eyes, and lungs even in very small concentrations. Exposure to 300 ppm is immediately life threatening. At concentrations of approximately 15 – 28 % by volume in air ammonia is also flammable. (OSHA, 2013).

1.2.4 Acetone

Acetone is the simplest and smallest ketone. Its formula is $(CH_3)CO$. Acetone is colourless, volatile, and highly flammable liquid in room temperature. Its melting point is at −94.7 ℃ and boiling point at +56.1 ℃. Acetones specific heat is 2.2 kJ/(kg·K). Acetone has been studied well and demonstrates only meager toxicity in normal use. United States food and drug administration has rated acetone as 'generally recognized as safe' (GRAS) when it is present in beverages, foods, and in preservatives at concentrations < 8 mg/l (Hernandez 1999). However, acetone is known to cause mild skin irritation and severe eye irritation and at high vapor concentrations in the air it may cause harm to central nervous system (CCOHS 1997).

1.2.5 R-134a – R1234yf

R-134a and R1234yf, or 1,1,1,2-Tetrafluoroethane and 2,3,3,3-Tetrafluoropropene respectively are both classified as refrigerants. These working fluids are commonly used in the refrigeration cycle of car and household air conditioning systems and heat pumps. One of the most notable differences in these two substances are their GWP (global warming potential). R-134a has a GWP of 1400 whereas in the case of R1234yf, it has a GWP of less than 1 (Cooling Post 2021). Tetrafluoroethane is one of the fluorinated greenhouse gases banned by the Kyoto Protocol. Therefore, R1234yf was chosen to replace R-134a. As of 2021, the use of R-134a was banned in the US in light duty vehicles and will be phased out from centrifugal and positive displacement chillers in 2024 (Johnson A, 2016).

1.2.6 Paraffin

Paraffin wax is colourless substance. It consists of a mix of hydrocarbons, which contain 20 – 40 carbon atoms. In room temperature it is solid, and it melts around 37 ℃. Paraffins specific heat capacity is 2.14 – 2.9 $\frac{\mathrm{kJ}}{\mathrm{kg \cdot K}}$ and heat of fusion ranges from 200 to 220 $\frac{\mathrm{kJ}}{\mathrm{kg}}$. The wax itself has poor heat conductivity, 0.2 $\frac{\mathrm{W}}{\mathrm{m \cdot K}}$, so effective use as a heat storage would require finned containers to increase the heat removal rate from the system. The wax is made from petroleum, coal, or oil shale.

Table 1.1 Various thermophysical properties of the substances discussed above. (Engineering toolbox 2021), (Lumitos Ag 2022), (Usman M. et al. 2020), (Climatelife 2018), (Suberu J. et al. 2016), (Chemours FC 2018).

	Specific heat capacity							
	solid	liquid	gas	Heat of evaporation at boiling point	Heat of fusion	melting point	boiling point	Thermal conductivity
	[kJ/kg K]	[kJ/kg K]	[kJ/kg K]	[kJ/kg]	[kJ/kg]	[°C]	[°C]	[W/m °C]
Acetone	N/A	2.14	1.29	534	98	-94.9	56.1	0.18
Ammonia	N/A	4.744	2.175	1372	332	-77.7	-33.3	0.02
Methanol	N/A	2.53	2.95	1165	99	-97.6	64.7	0.20
Paraffin	2.14 - 2.9	N/A	N/A	N/A	200 - 220	47 - 64	370	0.2
R1234yf	N/A	1.392	0.905	160	N/A	N/A	-29.5	0.15
R-134a	N/A	1.354	N/A	195	N/A	-103.3	-26.1	N/A
Water	2.093	4.182	1.996	2256	334	0	100	0.598

2 SOLID-TO-LIQUID PHASE CHANGE MATERIAL APPLICATIONS

Solid phase change materials are usually used as a heat storage in applications where there is no need for heavy constant cooling and a high heat load is periodical. Solid PCMs are also favoured in situations where liquid cooling would take up too much space, as they usually need large radiators and other equipment to cool and move the cooling fluid through the system.

2.1 Paraffin based heat storages

Paraffin has been researched in use as a heat storage in housings (Sarbu I. 2018) and in electric motor applications with intermittent high load periods (Wang S. et al. 2016).
According to their FEM analysis Shengnan Wang et al. (2016) were able to extend their PMSM continuous power mode by 33 %. The modelled PMSM had a rated output power pf 2.5 kW.

The sealed in paraffin cavities need to have enough space in between them. Otherwise, paraffin would work as an insulation blocking the heat transfer, and possibly causing overheating. They ran simulations with twelve paraffin cavities with varying number of aluminium sheets, that divided those cavities into evenly spaced sections. These sheets were dividing the cavities through the length of the casing. Seen in figure 2.1.

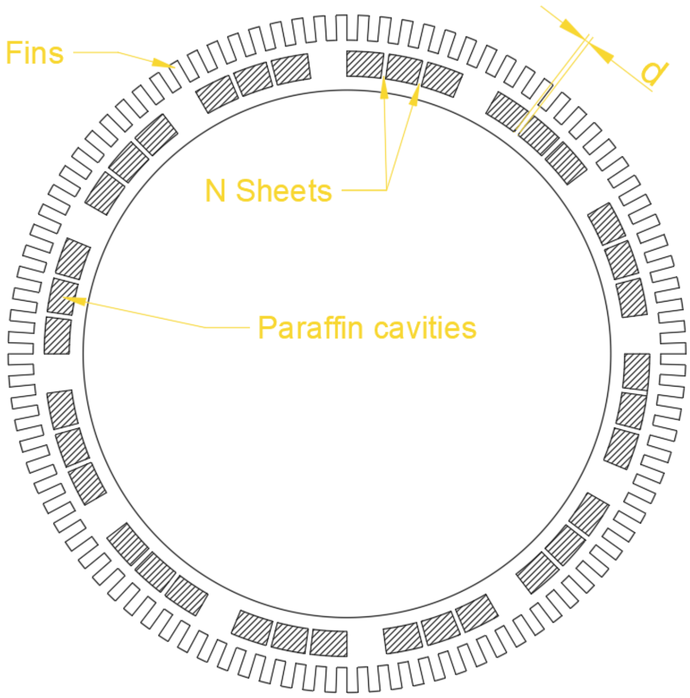

Figure 2.1 Cross-sectional view of the Wang S. et al. 2016 motor casing with paraffin cavities.

There were 5 different simulated casing variants shown in table below. The fifth variant was a case without paraffin cavities named case0, Table 2.1.

Table 2.1 Different case variants used in Wang S. et al. research.

Case #	1	2	3	4
Number of aluminium sheets	0	2	2	5
Sheet thickness d [mm]	0	1	0.5	0.5

They simulated each case configuration with both periodic and continuous heat load modes. The PMSM used in the simulation was designed to have insulation material class E, whose highest rated heat resistance is 393 K. According to Wang S. et al. based on their experience with PMSM with natural convection cooling the temperature difference between windings and the casing is approximately 15 – 20 K. Therefore, they set a maximum case temperature to 373 K after which the machine was considered to be overheated. Case0 reached this temperature in 1070 seconds. Case4 had the best performance out of the other variants keeping the case below 373 K under constant load for 1420 seconds, which in this case was a 32 % improvement over case0. Their results can be seen in figure 2.2.

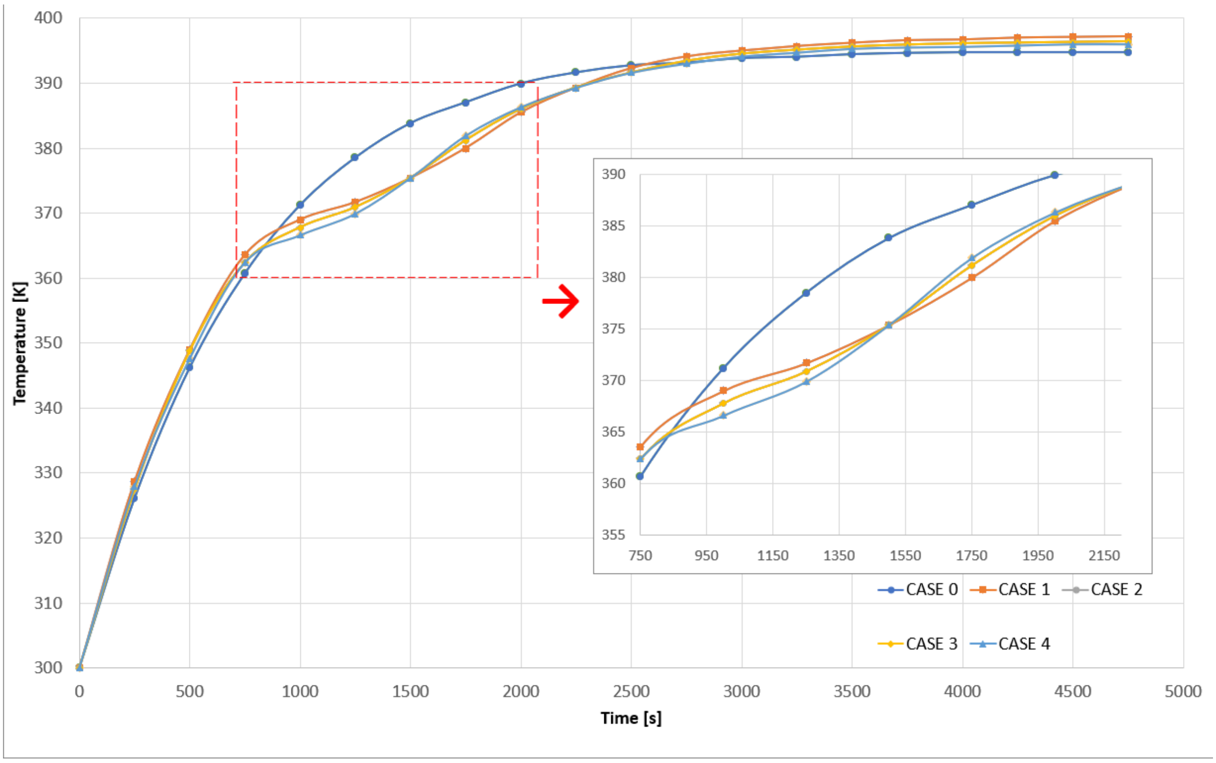

Figure 2.2 Temperature curves of aforementioned casings under constant 270 W heat load. Figure datapoints source: (Wang S. et al. 2016).

They also ran simulations with paraffin with different melting points ranging from 60 °C to 90 °C in 10 °C increments. The paraffin with melting point of 90 °C proved to be the most efficient from the other tested variants, and it was used when drawing the results in figure 2.2.

3 HEAT PIPES

Heat pipe is a two-phase heat transfer system, which consist of hermetically sealed copper or aluminium shell, heat transferring fluid, and a porous wick structure, which enables the movement of the cooling liquid through capillary action (Figure 3.1).

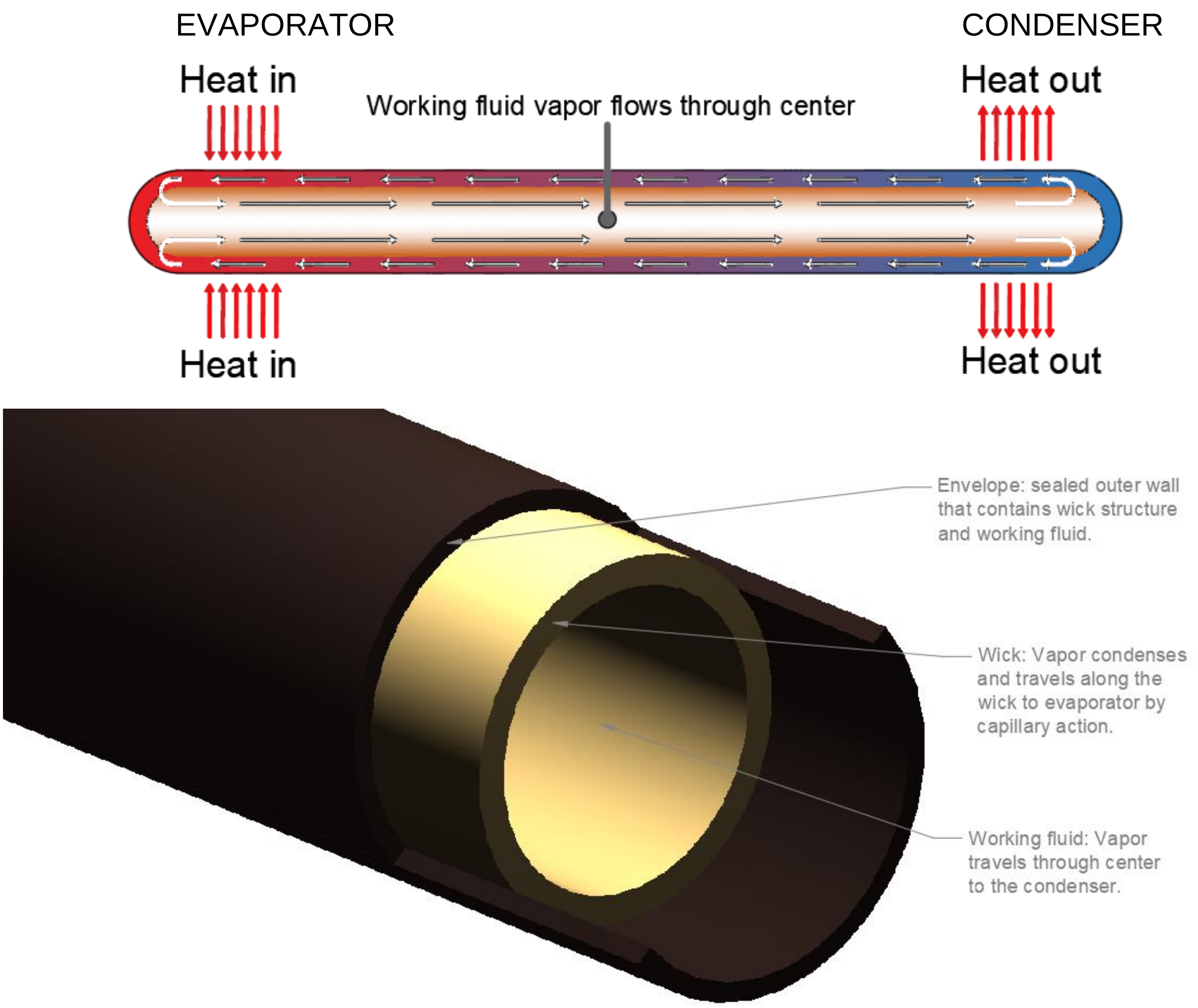

Figure 3.1 Heat pipe working principle.

The heat source evaporates the liquid inside the heat pipe in the evaporator from which the vapor is then transferred through the centre of the heat pipe to the condenser. In the condenser, the vapor condenses to liquid after which it is transferred via the wick back to the evaporator part of the heat pipe. Phase changing process and the dual-phase flow circulation persists as long as the temperature between these two parts differentiates enough. (1-ACT 2020).

Depending on the design of a heat pipe, in sub-zero conditions the fluid it contains may freeze. Start up in the frozen state may be problematic if the heat transfer and thermal mass of the system are such that the fluid in the evaporator side is thawed and vaporized by the thermal energy source while it freezes in the condenser side after the vapor travels there. This could lead into depletion of working fluid in the evaporator side, which would eventually shut down the heat pipe. This is usually not a problem for the heat pipe but rather a system design issue. There are essentially four different methods to combat this issue:

- Design a system where start up in a frozen state is not a concern, where the systems is capable of thawing the whole system all the way to the condenser side.
- Use an active control method, like shutting down fans to restrain heat energy transfer in sub-zero temperatures.
- Design a secondary heat transfer method to circumvent frozen heat pipes.
- Fill the heat pipe with fixed amount of non-condensable gas, which ensures the system can freeze and thaw completely without issues.

In most cases first and the third option are used. (1-ACT 2020).

The effectiveness of a heat pipe can be described with the thermal resistance. The thermal resistance R of heat pipe can be calculated with the following equation:

$$R = \frac{T_\mathrm{e} - T_\mathrm{c}}{Q}. \tag{3.1}$$

The overall heat transfer coefficient $[\frac{\mathrm{W}}{\mathrm{m}^2} \cdot \mathrm{K}]$ of a heat pipe can be solved by

$$h = \frac{Q}{A(T_\mathrm{e} - T_\mathrm{c})}, \tag{3.2}$$

Where Q is the heat input [W], A is the heat transfer surface of the area at the evaporator $[\mathrm{m}^2]$, T_e is the average temperature at the evaporator $[K]$ and T_c is the average temperature at the condenser $[K]$. (Mozumder A. et al. 2011).

The heat transfer coefficient of a heat pipe varies greatly over many different aspects of the entire cooling system such as, shape and size, alignment, pipe heat transfer fluid fill factor, the temperature at the condenser and at the evaporator, cooling method of the condenser, and the chosen cooling fluid inside the heat pipe. Ponnapan et al. 1998 managed to get their heat pipes heat transfer coefficient to 1.3 $\frac{\mathrm{kW}}{\mathrm{m^2K}}$. This was achieved by spray jet oil cooling the condenser. Their research will be talked more in depth in the next section.

Kumar V. et al. 2007 did research about heat pipe inclinations effect on its heat transfer rate. They managed to reach a heat transfer coefficient of 696 $\frac{\mathrm{W}}{\mathrm{m^2 \cdot K}}$. The heat pipe dimensions were 800 mm length, 25.4 mm OD and 22 mm ID. The condenser had annular fins that had a 50.8 mm diameter with 0.3 mm thickness.

3.1 Rotating heat pipes

Like conventional heat pipes, rotating heat pipes (RHPs) consist of three different sections: Evaporator, adiabatic and condenser section. Most RHPs transfer heat axially, but there are RHP types, which transfer heat in radial directions. While the axial type RHP does work without inner taper, its operation is enhanced when such taper is present (Reay D. et al. 2014). An example schematic of tapered RHP can be seen below.

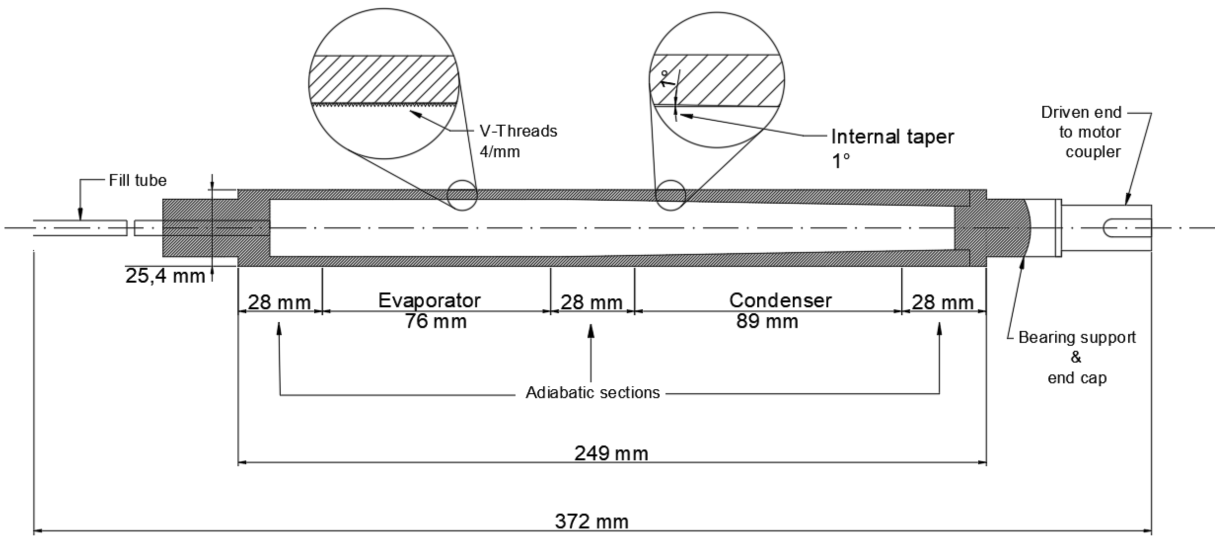

Figure 3.2 An example rotating heat pipe with tapered condenser. (Ponnapan R. 1998).

Typically, rotating heat pipes (RHPs) use their inner conical shape and centrifugal force to drive the cooling fluid towards the evaporator, which can be utilized in a range of different rotating systems and machinery. (Wenlei L. et al. 2019). Because of the use of centrifugal force, there is no need for a wick structure.

High-speed rotating heat pipe (HSRHP) with tapered condenser was built and tested by Ponnapan R. et al. in 1998 with promising results. With 24.9 cm long and 2.54 cm outer diameter rotating heat pipe (Figure 3.7) they were able to transfer 1kW of heat energy away from a switched reluctance machine rotor by spraying the heat pipe condenser section with oil. The maximum rotating speed of the rotor was 32000 rpm. The maximum convective heat transfer coefficient for the external cooling of the condenser they got was 1230 W/(m^2 K).

Ponnapan (1998) calculated their HSRHP's heat transfer coefficient h_{c} using a following formula:

$$Q_{\mathrm{cal}} = h_{\mathrm{c}} A_{\mathrm{c}} (T_{\mathrm{c,av}} - T_{\mathrm{f}}), \tag{3.3}$$

Where Q_{cal} was heat removed by oil [W], $T_{\mathrm{c,av}}$ was the average temperature of the condenser and T_{f} was the temperature of oil inlet. When calculating the heat pipe heat transfer coefficient using equation (3.2) provided by Mozumder A. et al., the result for the evaporator $h = 6.5\,\mathrm{kW/(m^2K)}$. The parameters used: The heat input $Q = 750\,\mathrm{W}$, evaporator area $A = 0.0061\ \mathrm{m}^2$, and temperature difference between evaporator and condenser $\Delta T = 19\ K$.

This highlights a key limiting factor in rotating heat pipe setups, which is the heat dissipation in the condenser part. In Ponnapan's (1998) research test setup, they were able to dissipate 1. 3 kW of heat energy away from the system thanks to an oil jet. The maximum volume flow for the oil used in their test was 3.22 litres per minute, and it was sprayed on the condenser from a single nozzle. The heat pipe's capacity to remove heat with air cooling alone was significantly lower. The total air flow of 14.87 m^3/h through three spigots kept 120 degrees apart around the heat pipe. Figure 3.3 bellow shows the external condenser heat transfer coefficients.

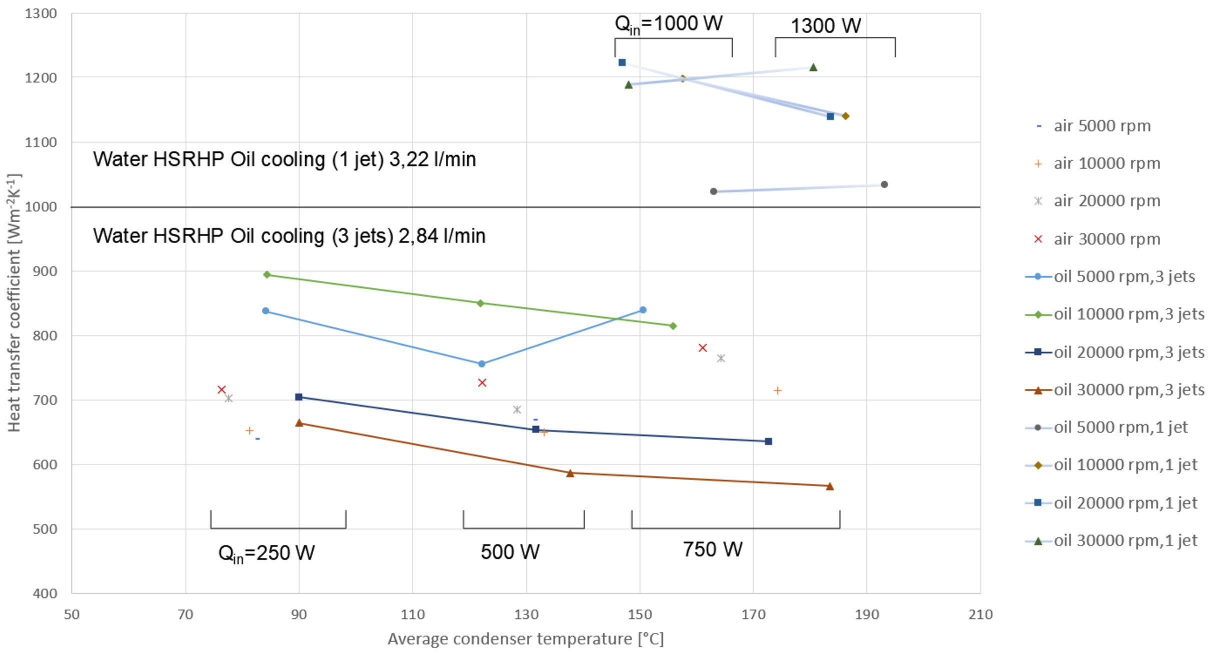

Figure 3.3 External condenser heat transfer coefficients in Ponnapan's research test setup with air and oil spray cooling. (Ponnapan R. 1998)

In the figure one can deduce, that while air cooling could be used in certain applications, and spray cooling the condenser with oil is almost twice as effective.

3.2 Gas-loaded heat pipes

Usually, non-condensable gas in a heat pipe is detrimental to its capability to remove heat from a source (Shuang-Fei L. et al. 2020), but on certain cases non-condensable gas can be utilized in heat pipes to tweak it's intended behaviour in more fluctuating environments.

Gas-loaded heat pipes, which are also known as variable conductance heat pipes (VCHP) use non-condensable gas to adjust the active length of the condenser i.e., the part of the condenser that is actively working to remove heat away from the source. The non-condensable gas may also be used to aid in start-up from and shutdown to a frozen state. (1-ACT 2022).

In such heat pipes the non-condensable gas enables it to restart by blocking the condenser as the temperature decreases. When the temperature drops low enough, the heat pipe shuts down as the evaporation and condensing cycle stops. As the temperature decreases and nears the temperature which freezes the working fluid, the vapor pressure within the VCHP decreases. To preserve the equilibrium of the pressure at the vapor-gas interface, the non-condensable gas expands. The expansion decreases the condensers active length. This in turn both restricts the flow of vapour to the passive part of the condenser and maintains the active part of the condenser in a higher temperature than what would be in a normal heat pipe in similar conditions. When the working fluid reaches its designed limit temperature, the whole condenser will be taken up by non-condensable gas. Further drop in temperature beyond the shut off point will result in the non-condensable gas expanding to the adiabatic section of the heat pipe. Under normal conditions the working fluid will then freeze and reside mostly in the evaporator part and in the adiabatic part, which makes freezing start up easier. (1-ACT 2022).

The heat pipes described above work best when the condenser part of the VCHP is above the evaporator. These kinds of VCHPs have relatively short evaporators compared to their condensers, and the amount of non-condensable gas they contain is fixed. (1-ACT 2022).

Second kind of VCHPs have a valve at the top of the VCHP at the condenser side and a non-condensable gas storage which is equipped with a heater. This allows for more control over the active length of the condenser. When heating the gas storage, the non-condensable gas expands and pushes further into condenser part of the VCHP. (Law R. et al. 2018).

3.3 Heat pipe material and working fluid

The choice of heat pipe material and the cooling fluid combination is important, since wrong combination may produce a heat pipe performance reducing reactions, such as heat pipe inner wall corrosion. These reactions may also produce non-condensable gasses inside the heat pipe, which will reduce heat pipes heat transfer capabilities notably. In appendix 2 a table of various working fluids can be found.

According to Faghri A. 2014 a useful range of working fluids is when the saturation pressure is between 0.1 and 20 bar. When it is <0.1 bar there is not enough evaporation. When the saturation pressure is >20 bar, the heat pipe wall thickness must be increased to such extent that it becomes the main hindrance to the thermal conductance of the system.

When considering these vapor pressure restrictions, according to Faghri A. 2014, for example water’s working range would be 303-550 K, and for methanol it would be 283-403 K. Faghri A. 2014 assessments, however, seem to be for conventional heat pipes, since Ponnapan R. et al. 1998 were successfully transporting 750 W of heat power away from an evaporator of a methanol high-speed rotating heat pipe where its temperature rose as high as 473 K.

Anderson W. et al. 2007 tested copper/nickel and Monel heat pipes with Cesium as working fluid. They did life tests with monel (a copper/nickel alloy with small amounts of iron, manganese, carbon, and silicon) and copper/nickel 70/30 heat pipes with Cesium at 475 °C for 1000 hours. After 1000 hours the heat pipes were cut, and their inner surface was examined. Results showed clear signs of heat pipes inner surface deterioration. Copper build-up could be clearly seen in the heat pipe’s evaporator section area. In time this would have clogged up the wick structure, which in turn would significantly hamper the performance of the heat pipe.

When the heat pipe structure and the cooling fluid react with each other, the reaction may produce non-condensable gasses inside the heat pipe. These gasses have an adverse effect on heat pipe’s heat transfer capabilities. According to Reay D. et al. 2014, non-condensable gasses can effectively block off condenser section it occupies, which then effectively stops all local heat transfer.

3.4 Heat pipe alignment

Heat pipes’ heat transfer efficiency is affected by its tilt angle. When condenser is cooled with forced convection, the fluid circulation inside the heat pipe becomes one of the primary catalysts for heat transfer. In this case vertical alignment would work best for the heat pipe as the fluid circulation inside the heat pipe becomes gravity assisted. In figure 3.4 there are measurements done by Abhat A. et al. 1976 of two different thermosyphons in different angles. The angles are measured form horizontal axis, and a clear correlation can be seen in between heat pipe angle and maximum heat removed from the source.

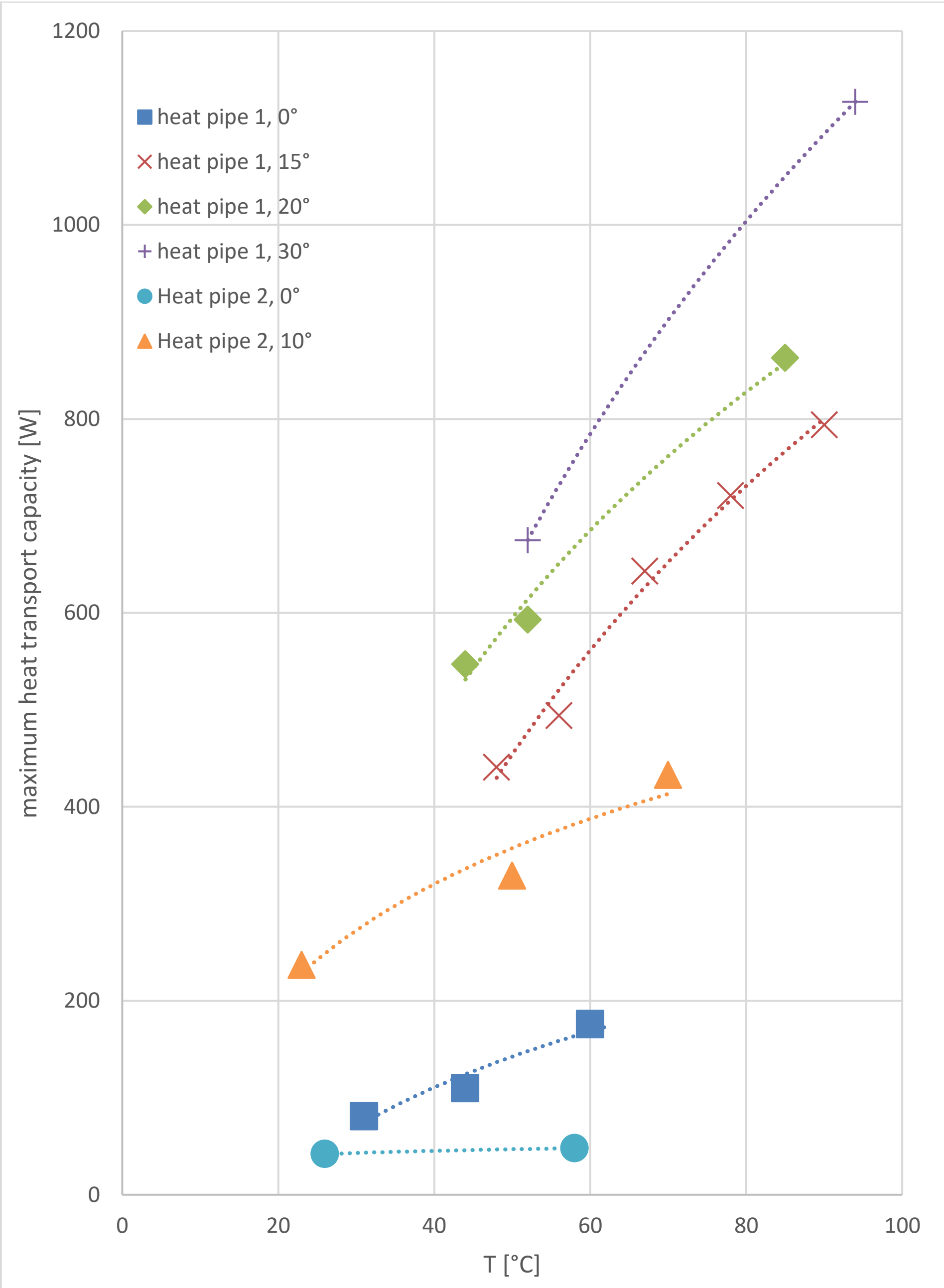

Figure 3.4 Tilt angle's effect on certain water filled heat pipes' performance. Angle measured from horizontal axis. (Abhat A. et al. 1976).

When both heat pipes are level with horizontal axis, their heat transfer capabilities drop tremendously as half of the cooling liquid inside resides at the condenser part of the heat pipe. This rises the thermal resistance of those heat pipes.

In case of natural convection, the alignment of outside fins on the condenser become a significant factor in heat pipe heat transfer rate as per Kumar et al. 2007. They had an experimental setup where the evaporator of a heat pipe was heated with circulating warm water. The heat pipe was mounted on a contraption with which the angle of the heat pipe and the heating element could be measured and changed. A diagram of their testing rig can be seen in figure bellow.

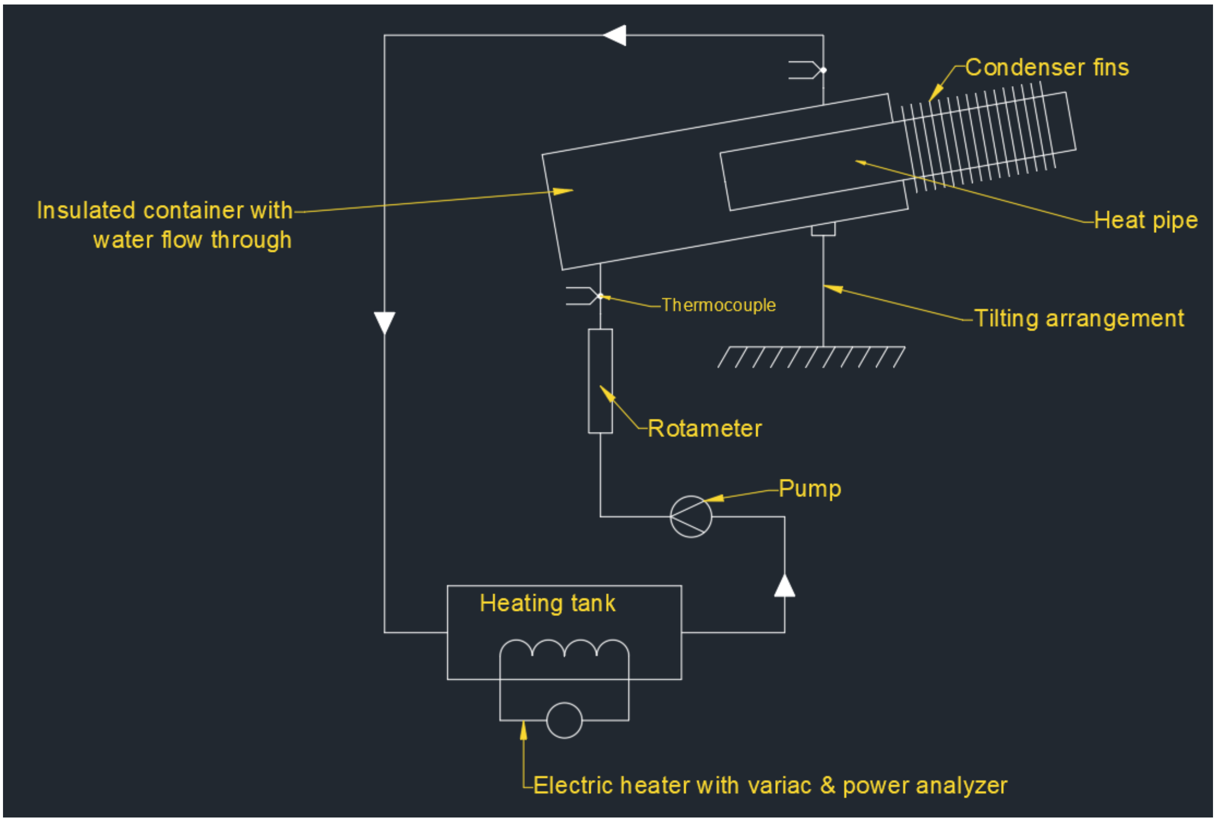

Figure 3.5 Kumar et al. 2007 diagram of testing rig for their heat pipe.

The evaporator side of the heat pipe was encased in a cylindrical casing made of galvanized iron, which in turn was surrounded by glass wool. Hot water was used to supply the heat pipe with thermal energy. Its dimensions were 800 mm long and its outer diameter was 25.4 mm. The condenser part of the heat pipe was 400 mm long and had 41 annular aluminium fins with 50.8 mm diameter and 0.3 mm thickness at a pitch of 9 mm (Figure 3.6).

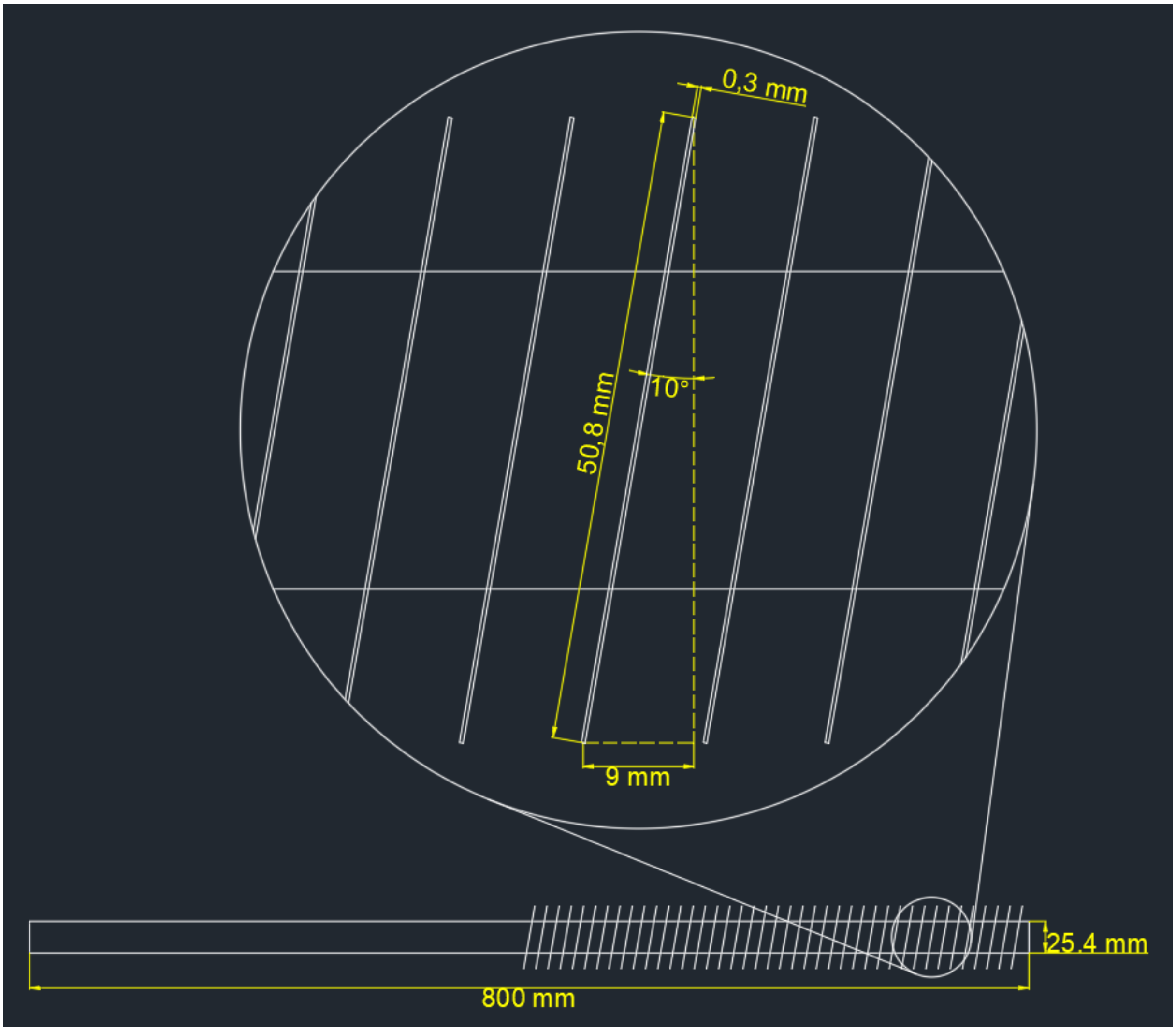

Figure 3.6 Some dimensions of the heat pipe used in Kumar et al. 2007 research test setup.

They did multiple tests with different heating fluid temperatures in several tilt angles. The results can be seen in figure 3.7.

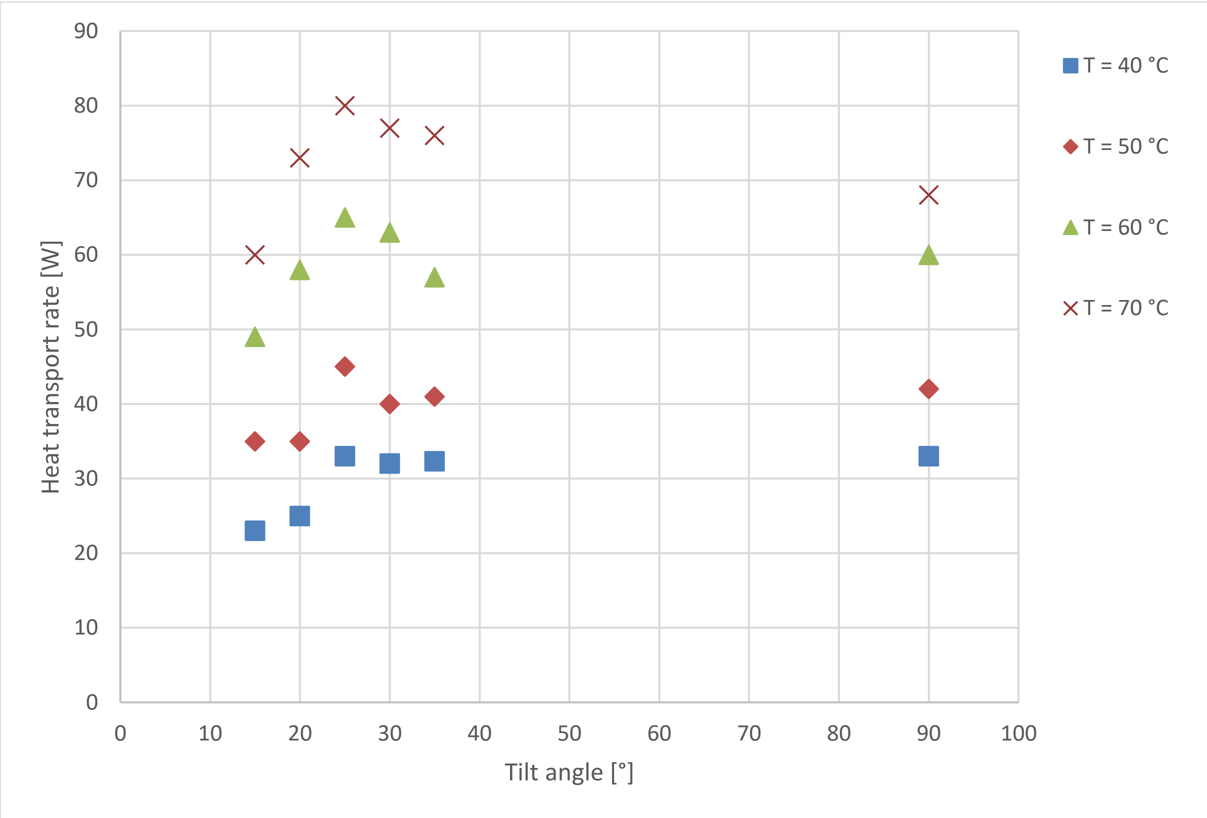

Figure 3.7 Tilt angle, and its effects on the thermal performance of the heat pipe on Kumar et al. 2007 research.

Their research concluded that their heat pipe transferred the most heat energy when the heat pipe was aligned in 25 ° angle from the horizontal axis. While the fill factor of the heat pipe was not mentioned in the research, it could be possible that in lower inclinations the water inside the heat pipe was blocking part of the condenser, which in turn resulted in increased thermal resistance for the heat pipe and therefore lowered its heat transport rate. After 25° tilt angle the reason for the drop in its heat transport rate could be that the angle on the condenser fins start to hamper efficient natural convection air flow through the fins.

3.5 Heat pipe fill factor

Heat pipe fill factor, or filling ratio, has a sizeable impact on the thermal resistance of a heat pipe. The fill factor is calculated by dividing the volume of the used fluid by the inner volume of the heat pipe. The optimal fill factor depends on the type of the heat pipe, the size of the heat pipe, and the designed heat input for the heat pipe (Shuang-Fei L. et al. 2020). For instance, optimal fill factor for a rotating heat pipe is usually below 0.2 (Song F. et al. 2003) (Ponnapan R. et al. 1998), while for certain pulsating heat pipes it is closer to 0.6 (Babu E.R. et al. 2017). For a conventional thermosyphon with finned condenser Kumar V. et al. 2007 used a following equation to calculate required fluid inventory amount *M* in kilograms:

$$M = A_{\mathrm{V}} L_{\mathrm{t}} \rho_{\mathrm{V}} + A_{\mathrm{W}} L_{\mathrm{t}} \varepsilon_{\mathrm{o}} \rho_{\mathrm{l}}, \tag{3.4}$$

Where A_{V} is vapor core area [m^2], L_{t} is total length of the heat pipe [m], ρ_{V} is vapor density, A_{W} is wick surface area, ε_{o} is porosity of wick material, and ρ_{l} is density of liquid water inside the heat pipe.

For rotating heat pipes determining the optimal fill factor is a complicated matter. It depends on the inner shape of the heat pipe. Vasilev L. et al. 1983 researched rotating heat pipes with cylindrical condenser with longitudinal grooves. They calculated minimum fluid film thickness required to maintain good thermal conductance inside the heat pipe. Ponnapan R. 1996 modified Vasilev’s given expression for tapered rotating heat pipe:

$$\delta = \left[\frac{Q^2}{4\pi^2 (\Omega^2 r_{\mathrm{m}} - g) \sin \alpha r_{\mathrm{m}} \rho_{\mathrm{f}}^2 h_{\mathrm{fg}}}\right]^{0,25} \tag{3.5}$$

Where Q is heat input load [W], Ω is mechanical angular velocity [rad/s], r_{m} is the mean radius of taper section [m], α is the half cone angle of taper in the condenser, ρ_{f} is fluid density [kg/m^3], and h_{fg} is latent heat of vaporization [kJ/kg]. From the expression above one can infer that the required fluid inventory increases as the heat input increases, while increase in rotational speed or increase in heat pipe inner diameter decreases the optimal filling ratio.

4 HEAT PIPE POSITIONING

There are several apt locations for heat pipes in electrical machines. Both stator and rotor produce heat that needs to be transferred away from the machine.

4.1 Rotor

Keeping the rotor below certain temperature is essential for an electrical machine to work properly. Too high rotor temperatures can potentially damage the system, the rotor coils or destroy its permanent magnets in case of permanent magnet synchronous machine. Therefore, a heat pipe at the centre of the rotor or multiple heat pipes located near the centre of the rotor axis could be used to transfer heat energy away from the system.

The utilization of multiple heat pipes outside the rotor centre line has been researched before by M. Groll et al. in 1978, where an asynchronous motor's rotor model was fitted with 6 copper/water heat pipes. An example is shown in figure 4.1. The test was run with heat pipes with and without capillary structure. The transferred heat was dissipated from both sides of the model rotor with forced convection cooling (20 m/s).

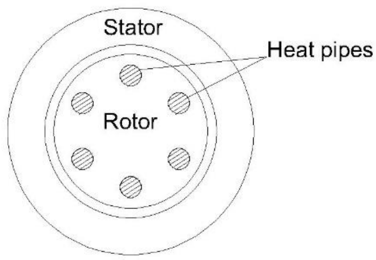

Figure 4.1 An example of a heat pipe arrangement where heat pipes are not in the centre of the rotor axis.

In Groll's arrangement their rotor had twelve axial boreholes, into six of which heat pipes were brazed. They were able to transfer 500 W of heat energy per heat pipe. The maximum rotor speed in their test setup was 6000 rpm. The heat pipes were 700 mm long, had a 25 mm outer diameter, and a 10 mm inner diameter. The heat pipe axis and rotor axis were 10 cm apart. While in motion, there was not a significant difference between heat pipes with and without capillary structure. However, during standstill the heat transport capacity heat pipes without capillary structure proved to be insufficient. The helically grooved heat pipes, on the other hand, cooled the rotor effectively at low rpm and at standstill.

More conventional heat pipe arrangement is to install it in the centre of the rotor. This way the heat pipe benefits the most from the rotation of the rotor, where the fluid inside the heat pipe can form a near uniform film around the heat pipe evaporator zone provided the rotor revolves with high enough frequency, and the heat pipe fill ratio is close to optimal. According to Petersson and Wu 1991 a liquid annulus forms, when on-axis rotational acceleration exceeds $20g$ ($g = 9.81\,\frac{\mathrm{m}}{\mathrm{s}^2}$), and when formed it collapses after the acceleration declines bellow $10g$. An example model is represented in figure 4.2 below.

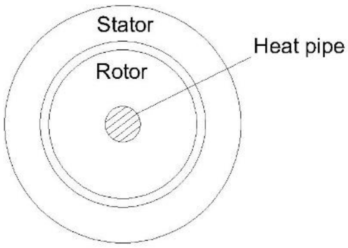

Figure 4.2 An example of typical placement position for a rotating heat pipe in the centre of a rotor.

This kind of an arrangement works well with high-speed applications, since the stresses from the rotor rotation are smaller in the centre of the rotor compared to the rotor's outer regions. Ponnapan R. 1998 designed such a heat pipe (249 mm length, 25.4 mm OD) that was meant to be installed in the rotor centre and managed to remove 1 kW of heat energy with it.

4.2 Stator

Stator windings produce a significant amount of heat during operation. If their temperature rises too high, the winding insulations could be damaged. Geng W. et al. (2021) made an experimental setup in 2021 where they inserted heat pipes into the middle of stator slots of an outer-rotor permanent magnet starter/generator (OR-PM S/G). Example figures below.

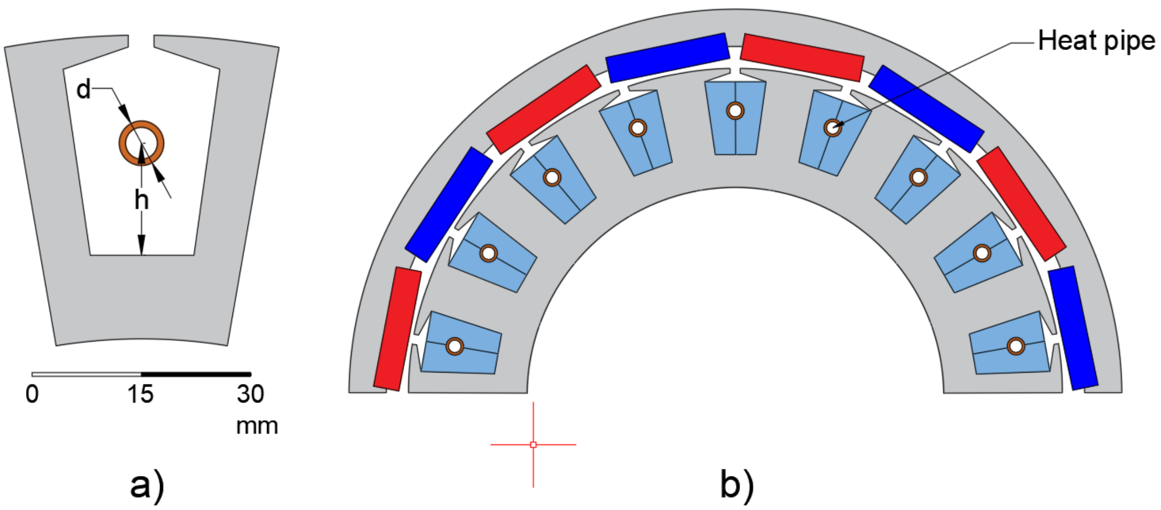

Figure 4.3 Geng W. et al. 2021 OR-PM S/G model with heat pipe in the slot. The total slot height was 30 mm.

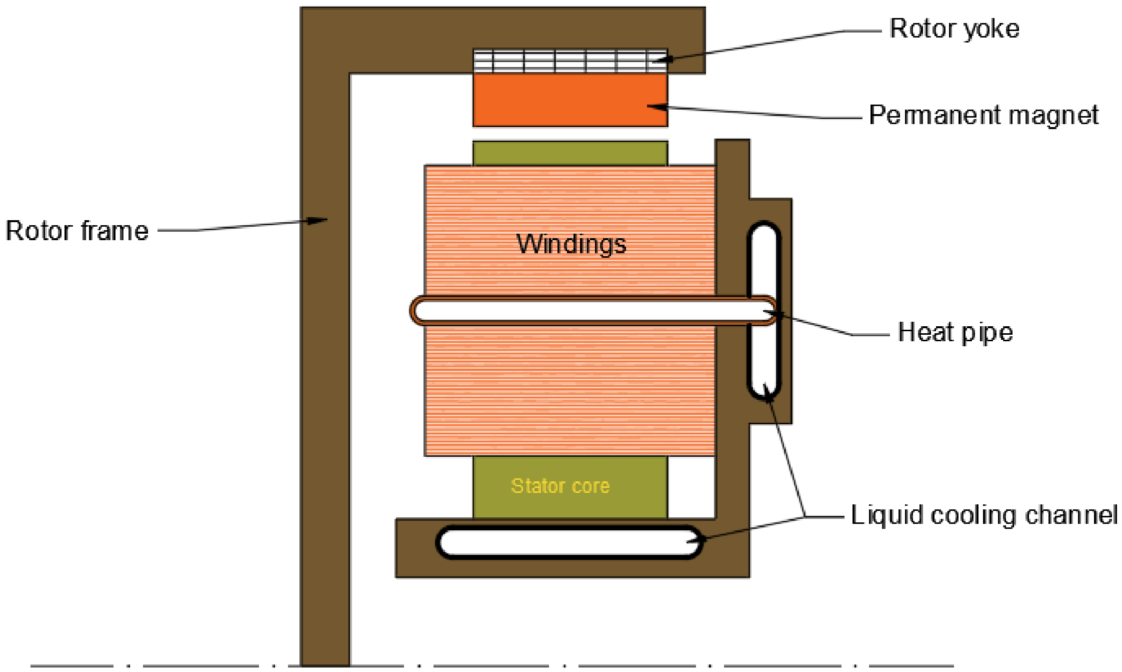

Figure 4.4 Geng W. et al. 2021 proposed method of cooling the OR-PM S/G.

Part of their research was to study the key parameters in Fig. 4.3 a), and their effects on loss distribution and thermal design. They found out that the heat pipe performed best when it was situated near the slot opening. Geng W. et al. 2021 stressed, however, that thorough analysis should be done to achieve optimal heat pipe size and separation distance from the slot opening. For their system, in their mathematical model, the optimal distance from the slot bottom was 18 mm. The slot total hight was 30 mm.

According to their calculations and measurements, compared to conventional water-jacket cooling, with their heat pipe arrangement the starter/generator was able to produce 25 % more output power due to improved cooling. With their final hybrid cooling arrangement of their OR-PM S/G where the heat pipes’ condenser section was embedded in the water-jacket, they were able to improve its output power by 60 % compared to arrangement without heat pipes.

5 SUMMARY

Some available technologies and research about electrical machine cooling utilized were highlighted. Heat pipes were studied more in depth, and paraffin use as a heat storage was briefly discussed. Several papers have found out that phase change materials in heat pipes and heat storages can be used as an effective way of cooling an electrical machine.

Ponnapan R. 1998 proved that high-speed rotating heat pipes with oil-spray cooling could be used to remove a significant amount of thermal energy with a relatively compact system, which reached 1 kW of heat transfer rate with water filled RHP that was about 40 cm long. A significant part of their research was concentrated in the heat removal from the condenser, which seems to be the limiting factor in RHP heat removal systems.

Anderson W. 2007 highlighted the importance of pairing the right heat pipe material with the right working fluid, as their life test experiments showed how certain combinations could erode the inside of the heat pipe and the wick structure. They ran life tests on monel heat pipes with caesium working fluid at 475 °C for 1000 hours. The test displayed notable deterioration and Anderson noted that in time the whole wick structure could have been blocked by copper build up.

Heat pipe position in the stator and rotor was also discussed. Groll M. et al. 1978 had tested heat pipe performance non-centred rotor heat pipes, which were 10 cm off rotor axis, could withstand rotation speeds of 6000 rpm at maximum. At the centre of the rotor heat pipes, i.e., what Ponnapan R. 1998 tested, could tolerate tens of thousands of revolutions per minute. In the stator side Geng W. 2021 had done extensive research on OR-PM S/G stator cooling, and one of the main points in their research was finding the optimal heat pipe diameter and the distance from the stator slot bottom for their outer rotor permanent magnet starter/generator.

Kumar V. et al. 2007 and Abhat A. et al. 1976 discussed about the importance of tilt angle for normal gravity assisted heat pipes. Both papers concluded that gravity assisted heat pipes work better at an angle from horizontal axis.

Paraffin-based thermal storage was researched by Shengnan Wang et al. (2016). They added paraffin cavities to their PMSM casing and with it the motor could run in continuous power mode for 33 % longer than a similar motor without paraffin cavities in its casing.

SOURCES

1-ACT. Advanced cooling technologies. Heat pipe reliability guide [WWW-document]. [referenced 27.1.2021]. Available at: https://go.1-act.com/ebook_heatpipe

1-ACT. Advanced cooling technologies. Heat pipe design guide: Frozen start-up. [WWW-document]. [referenced 15.10.2021]. Available at: https://www.1-act.com/resources/heat-pipe-design-guide/frozen-start-up/

1-ACT. Advanced cooling technologies. Gas loaded heat pipes for start up from a frozen state. [WWW-document]. [referenced 20.4.2022]. Available at: https://www.1-act.com/resources/heat-pipe-fundamentals/different-types-of-heat-pipes/gas-loaded-variable-conductance-heat-pipes-for-start-up-from-a-frozen-state/

A. Abhat, H. Nguyen-chi, Investigation of performance of gravity assisted copper-water heat pipes, in: Proceedings of the Second International Heat Pipe Conference, Bologna; ESA Report SP112, vol. 1, 1976.

Anderson W. et al. 2007. Intermediate Temperature Fluids Life Tests – Experiments. [WWW-document]. [referenced 27.5.2021]. Available at: https://www.researchgate.net/publication/235129503_Intermediate_Temperature_Fluids_Life_Tests_-_Experiments

Babu E.R. et al. 2017. Effect of Filling Ratio on Thermal Performance of Closed Loop Pulsating Heat Pipe. [WWW-document]. [referenced 5.5.2022]. Available at: https://www.sciencedirect.com/science/article/pii/S2214785318317218

Bin X. et al. 2017. Study on Overload Performance Enhancement of Motor Based on Heat Storage of Phase Change Paraffin. [WWW-Document]. [Referenced 12.1.2022]. Available at: https://ieeexplore.ieee.org/document/8056106

CCOHS, Canadian centre for occupational health and safety. 1997. Acetone. [WWW.document]. [Referenced 25.2.2022] Available at: https://www.ccohs.ca/oshanswers/chemicals/chem_profiles/acetone.html

Chemours FC 2018. Refrigerant (R-134a). [WWW-Document]. [Referenced 30.5.2022] Available at: https://www.freon.com/es/-/media/files/freon/freon-134a-si-thermodynamic-properties.pdf?rev=7519d264dfd74fe68c04c9e119f7361f

Climatelife 2018. R-1234yf 2,3,3,3-tetrafluoroprop-1-ene.[WWW-Document]. [Referenced 30.5.2022] Available at: https://climalife.dehon.com/uploads/product/media/document/r1234yf-fd-en-18.pdf

Cooling Post. 2021. IPCC confirms HFO GWPs are less than 1. [WWW-Document]. [Referenced 1.11.2021]. Available at: https://www.coolingpost.com/world-news/ipcc-confirms-hfo-gwps-are-less-than-1/

Dean, W. G.; Karu, Z. S. (February 1993). Space Station thermal storage/refrigeration system research and development.

Engineering ToolBox, (2018). Acetone - Thermophysical Properties. [WWW-Document]. [Referenced 30.5.2022] Available at: https://www.engineeringtoolbox.com/acetone-2-propanone-dimethyl-ketone-properties-d_2036.html

Geng W. et al. 2021. Windings Indirect Liquid Cooling Method for a Compact Outer-Rotor PM Starter/Generator with Concentrated Windings. DOI 10.1109/TEC.2021.3084507, IEEE Transactions on Energy Conversion.

Goddard Space Flight Center. 1999. Ammonia-Charged Aluminum Heat Pipes with Extruded Wicks. [WWW-Document]. [Referenced 25.10.2021]. Available at: https://llis.nasa.gov/lesson/698

Groll M., et al. Heat pipes for cooling of an electric motor, Paper 78-446, in: Proceedings of Third International Heat Pipe Conference, Palo Alto, CA, AIAA Report CP784, New York, NY, 1978.

Hernandez O. 1999. Acetone: SIDS Initial Assessment Report (SIAR) for the 9th SIAM. [WWW.document]. [Referenced 25.2.2022] Available at: https://web.archive.org/web/20140309040008/http://www.inchem.org/documents/sids/sids/67641.pdf

Johnson A. 2016. Does R-134a Have a Phase Out Date? [WWW-document]. [Referenced 15.2.2022]. Available at: https://refrigeranthq.com/does-r-134a-have-a-phase-out-date/

Kumar V. and Dasaroju G. 2007. Heat Transfer Studies of a Heat Pipe. [WWW-document]. [Referenced 11.3.2022]. Available at; https://www.researchgate.net/publication/244588248_Heat_Transfer_Studies_of_a_Heat_Pipe

Law R. et al. 2018. Experimental investigation into the feasibility of using a variable conductance heat pipe for controlled heat release from a phase-change material thermal store. *Thermal science and engineering progress 7 (2018)* p. 125-130.

Lumitos AG 2022. Paraffin. [WWW-Document]. [Referenced 30.5.2022] Available at: https://www.chemeurope.com/en/encyclopedia/Paraffin.html

Mozumder A., Chowdhury M. & Akon A. 2011. Characteristics of Heat Transfer for Heat Pipe and Its Correlation. p. 3.

OSHA 2013, Ammonia refrigeration. [WWW-document]. [Referenced 29.10.2021]. Available at: https://www.osha.gov/ammonia-refrigeration

Peterson G. P., and Wu, D., "A Review of Rotating and Revolving Heat Pipes", American Society of Mechanical Engineer, Paper 91-HT-24, July 1991.

Ponnapan R. and Het Q. 1998. Test Results of Water and Methanol High-Speed Rotating Heat Pipes. JOURNAL OF THERMOPHYSICS AND HEAT TRANSFER Vol. 12, No. 3, July—September 1998

Ponnapan R. 1996. THERMAL MANAGEMENT RESEARCH STUDIES VOLUME 2 - ROTATING HEAT PIPE. [WWW-document]. [Referenced 6.5.2022]. Available at: https://apps.dtic.mil/sti/citations/ADA325412

Reay D. et al. 2014. Heat pipes theory, design and applications, 6th edition. ISBN: 978-0-08-098266-3.

Sarbu I. et al. 2018. A Comprehensive Review of Thermal Energy Storage. [WWW-document]. Referenced [11.1.2022]. Available at: https://www.mdpi.com/2071-1050/10/1/191/pdf

Shuang-Fei L. and Zhen-hua L. 2020. Parametric study of rotating heat pipe performance: A review. [WWW-document]. [referenced 30.3.2021]. Available at: https://www.sciencedirect.com/science/article/abs/pii/S1364032119306902

Socaciu, L., 2012. Thermal Energy Storage with Phase Change Material. Leonardo Electronic Journal of Practices and Technologies 11, 75–98.

Suberu J. et al., 2016. Feasibility of Using 2,3,3,3-Tetrafluoropropene (R1234yf) as a Solvent for Solid–Liquid Extraction of Biopharmaceuticals [WWW-Document]. [Referenced 30.5.2022] Available at: https://pubs.acs.org/doi/10.1021/acssuschemeng.5b01721

Usman M. et al., 2020. Improvement of thermal conductivity of paraffin wax, a phase change material with graphite powder. [WWW-Document]. [Referenced 30.5.2022] Available at: https://ieeexplore.ieee.org/document/9044541

Wang S. et al. 2016. Transient cooling effect analyses for a permanent-magnet synchronous motor with phase-change-material packaging. [WWW-document]. Referenced [11.1.2022]. Available at: https://www.sciencedirect.com/science/article/abs/pii/S1359431116313825

Wenlei L. & Taoyi H. 2019. Flow and heat transfer in a rotating heat pipe with a conical condenser. [WWW-document]. [referenced 19.3.2021]. Available at: https://www.sciencedirect.com/science/article/abs/pii/S073519331830263X?via%3Dihub

Xiong B. et al. 2017. Study on Overload Performance Enhancement of Motor Based on Heat Storage of Phase Change Paraffin. [WWW-document]. [referenced 7.5.2021] Available at: https://ieeexplore.ieee.org/document/8s056106

Appendix 1. Various working fluids for the heat pipe

Working fluid	Formula	Melting point at 1 bar, abs		Boiling point at 1 bar, abs		Critical temperature		Critical pressure
		[K]	[°C]	[K]	[°C]	[K]	[°C]	[bar, abs]
Ammonia	NH_3	196	-78	240	-33	406	133	111
Pentane	C_5H_{12}	143	-130	309	36	470	197	33
Acetone	C_3H_6O	180	-93	329	56	508	235	4,6
Methanol	CH_3OH	175	-98	338	65	513	240	80
Flutec PP2	C_7F_{14}	223	-50	349	76	486	213	20
Ethanol	C_2H_5OH	159	-114	352	79	516	243	62
Heptane	C_7H_{16}	183	-91	372	99	541	268	27
Water	H_2O	273	0	373	100	647	374	218
Toluene	C_7H_8	178	-95	384	111	865	592	41
Naphthalene	$C_{10}H_8$	353	80	490	217	748	475	40
Dowtherm	$C_{12}H_{10}O.C_{12}H_{10}$	285	12	527	254	770	497	30,9
Mercury	HG_2	234	-39	630	357	1750	1477	1720
Sulphur	S	386	113	718	445	1314	1041	207
Caesium	Cs	302	29	943	670	2045	1772	93
Rubidium	Rb	313	40	959	686	1938	1665	158
Potassium	K	336	63	1032	759	2223	1950	158
Tin Tetrachloride	$SnCl_4$	240	-33	388	115	592	319	37
Titanium Tetrachloride	$TiCl_4$	243	-30	410	136,6	638	365	46
Aluminum Tribromide	$AlBr_3$	370	97	528	255	763	490	86
Eutectic Diphenyl/Diphenyl Oxide		285	12	530	257	770	497	31
Antimony Tribromide	$SbBr_3$	370	97	553	280	1178	905	55